Mechanochemistry of Protein 4.1's Spectrin–Actin-Binding Domain: Ternary Complex Interactions, Membrane Binding, Network Integration, Structural Strengthening

Dennis E. Discher,*‡ Ricky Winardi,‡ P. Olivier Schischmanoff,‡ Marilyn Parra,‡ John G. Conboy,‡ and Narla Mohandas‡

*Joint Graduate Group in Bioengineering, University of California, Berkeley and San Francisco, California 94143; and ‡Life Sciences Division, Lawrence Berkeley Laboratory, University of California, Berkeley, California 94720

Abstract. Mechanical strength of the red cell membrane is dependent on ternary interactions among the skeletal proteins, spectrin, actin, and protein 4.1. Protein 4.1's spectrin–actin-binding (SAB) domain is specified by an alternatively spliced exon encoding 21 amino acid (aa) and a constitutive exon encoding 59 aa. A series of truncated SAB peptides were engineered to define the sequences involved in spectrin–actin interactions, and also membrane strength. Analysis of in vitro supramolecular assemblies showed that gelation activity of SAB peptides correlates with their ability to recruit a critical amount of spectrin into the complex to cross-link actin filaments. Also, several SAB peptides appeared to exhibit a weak, cooperative actin-binding activity which mapped to the first 26 residues of the constitutive 59 aa. Fluorescence-imaged microdeformation was used to show SAB peptide integration into the elastic skeletal network of spectrin, actin, and protein 4.1. In situ membrane-binding and membrane-strengthening abilities of the SAB peptides correlated with their in vitro gelation activity. The findings imply that sites for strong spectrin binding include both the alternative 21-aa cassette and a conserved region near the middle of the 59 aa. However, it is shown that only weak SAB affinity is necessary for physiologically relevant action. Alternatively spliced exons can thus translate into strong modulation of specific protein interactions, economizing protein function in the cell without, in and of themselves, imparting unique function.

T HE erythrocyte is among the simplest and best characterized of cellular systems within which the chemistry of composition can be intricately related to structural function. Indeed, most of the red cell's mechanical behavior, except for limited aspects of cell shape, appears to depend little on the complexities of intracellular metabolism (14). However, to withstand the forces of blood flow over a several-month lifespan, the erythrocyte's membrane components must assemble into a highly durable structure. Physical limits to this durability are set by the system's mechanochemistry, which is defined here as those molecular interactions that permit a pliable, yet resilient structure.

Spectrin, actin, and protein 4.1 are the principal structural proteins of the thin, cohesive skeletal network that underlies the red cell's lipid bilayer (3, 5, 19). The network formed by these highly conserved and pervasive proteins confers resilience and durability to the red cell's composite membrane (14, 16, 36, 44, 46). Mixtures of these network proteins also show that they can form very stable complexes in vitro (37) which at approximately micromolar protein concentrations can undergo a phase transition to a three-dimensional gel (7, 15, 49). In the formation of the basic ternary complex, protein 4.1 appears to play a crucial role in stabilizing spectrin cross-links between actin filaments. Consistent with cross-link reinforcement, red cells deficient in protein 4.1 possess membranes that fragment more readily than normal when exposed to high fluid shear (46, 51).

The crucial stabilizing function of protein 4.1 ($\sim$80 kD) localizes to a relatively small ($\sim$10-kD) spectrin–actin-binding domain (SAB)[1] (10) whose function recently has been shown to be strongly modulated at the genetic level by alternative splicing. The SAB isoform expressed in the erythrocyte is encoded by two exons that translate to an alternative NH$_2$-terminal 21–amino acid (aa) "cassette"

Address correspondence to Narla Mohandas, Mailstop 74-157, Lawrence Berkeley National Laboratory, 1 Cyclotron Road, Berkeley, CA 94720. Tel.: (510) 486-7029. Fax: (510) 486-6746.

---

1. *Abbreviations used in this paper:* aa, amino acid; FL-PE, fluorescein-phosphatidylethanolamine; GPI, glycosylphosphatidylinositol; GST, glutathionine-*S*-transferase; IAF, iodoacetimido-5-fluorescein; SAB, spectrin-actin-binding domain.

and a constitutive 59-aa domain (8, 25). Studies with recombinant isoform constructs of the SAB (11, 24) demonstrated that inclusion of the 21-aa cassette is critical for spectrin binding and also for efficient, 4.1-like activity in both ternary complex formation and membrane strengthening. Whether the 21-aa peptide, by itself, completely specifies these biochemical and biophysical properties was not addressed. Neither was it determined whether SAB isoforms lacking the 21aa are completely inactive, or simply much less efficient in some functions.

To dissect methodically such issues of protein functionality, COOH-terminal deletants of the SAB were constructed (see Fig. 1) and their functions characterized. We found that the 21 aa cassette plus 43 residues from the downstream sequence (peptide designation 21.43) are required for strong, 4.1-like interactions with spectrin and actin. Ternary complex formation in vitro, however, does not strictly require the 21 aa, but does need at least the first 26 residues of the downstream sequence in tandem with either the NH_2-terminal 21-aa cassette (to give a functional 21.26 peptide) or additional residues from the 59-aa domain (yielding a functional 0.59 peptide).

The physiological relevance of these in vitro results to both binding and mechanically strengthening intact membranes was also addressed. SAB peptide binding to normal membranes shows a highly specific, spectrin-dependent interaction. Integration of SAB peptide into a solidlike cytoskeletal network beneath the red cell bilayer is visually demonstrated by fluorescence imaged microdeformation (FIMD) (12). The strengthening effect of each SAB peptide on 4.1-deficient membranes is assessed in parallel with membrane binding; as found in vitro, the 21.43 is the most potent and effective at micromolar concentrations, while both the 21.26 and 0.59 are capable of strengthening membranes, but only at much higher peptide concentrations. The 21.20 is completely nonfunctional, even up to concentrations of ~250 μM. Since both the 21.26 and the 0.59, but not the 21.20 are functional, the first 26 residues appear to constitute an actin-binding site, and sequences flanking either side of this site seem essential for spectrin interactions. It therefore appears that actin binding in combination with even weak spectrin binding is sufficient, if not materially efficient, for network integration, stabilization, and structural strengthening.

Materials and Methods

Construction and Expression of SAB Peptides

SAB domain deletion constructs (Fig. 1) were generated from a minigene encoding slightly more than the SAB domain of erythroid protein 4.1 ($Glu^{400} \rightarrow Gly^{487}$) previously denoted 10k[21] (11). *Escherichia coli*–expressed peptides were either affinity purified as glutathione-S-transferase (GST) fusion peptides or cleaved off the GST moiety by digestion with thrombin (20). Additional constructs to those in Fig. 1 included a 21.41, a 21.36, and a 21.31. A fusion peptide with the *Xenopus laevis* SAB (Mays, K. T., R. Winardi, L. Zon, N. Mohandas, and J. G. Conboy. 1992. *Blood.* 80:273a.) was designated GST-XEN. Peptides were metabolically labeled by inducing the culture in a methionine-free minimal essential medium supplemented with [^{35}S]methionine and Luria broth (15% vol/vol). Primary structures were partially confirmed by immunoblotting (11). NH_2-terminal sequencing and mass spectrometry (Schischmanoff, P. O., unpublished data) further confirmed expression of the constructed sequences to within ~2 D. Peptide absorption spectra displayed the shapes expected (6) from
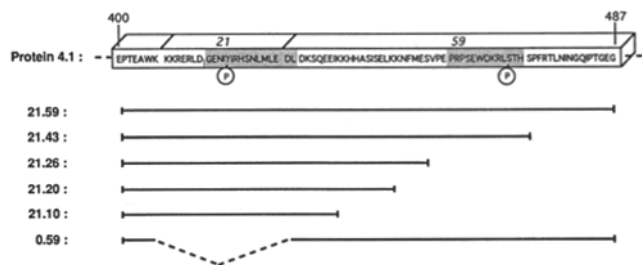
Figure 1. Deletion and isoform constructs of protein 4.1's SAB domain. The two gray regions show complete identity in sequence with the *X. laevis* SAB (Mays, K. T., R. Winardi, L. Zon, N. Mohandas, and J. G. Conboy. 1992. *Blood.* 80:273a). Within each of these two regions, at Tyr^{418} (45) and Ser^{467} (23), are sites for phosophorylation. Overall identity with *X. laevis* SAB is 75% with conservative amino acid substitutions accounting for the differences.

the relative Tyr and Trp composition; spectrophotometry was therefore used to quantify protein concentration (31).

Falling Ball Viscometry and Spectrin Composition of Networks

The ability of recombinant peptides to form a supramolecular complex with spectrin and actin was assayed by falling ball viscometry (9). Purified spectrin tetramer (40, 50) and rabbit muscle F-actin (38) were mixed (at 1.8 and 14 μM, respectively) and the recombinant peptide was subsequently added (up to ~250 μM). The solution was drawn quickly into a 50–100-μl microcapillary and assayed by falling ball viscometry as described elsewhere (11). For composition of spectrin–actin peptide networks, protein mixtures were either prepared directly in ultramicrofuge tubes or transferred from a microcapillary. Centrifugation, sometimes through a sucrose cushion, at 80 krpm, 22°C, for 7 min in a rotor (TLA-100; Beckman Instruments, Inc., Fullerton, CA) was followed by electrophoresis and densitometry (IS-1000; Alpha Innotech Corp., San Leandro, CA). Nearly all of the actin appeared in the pellets.

Actin Filaments Cosedimentation Assay

Fusion or thrombin-cleaved, ^{35}S-labeled proteins were incubated in thick-walled, ultramicrofuge tubes with a mixture of spectrin (2 μM) and actin (7 μM) in parallel with a control tube having the same amount of peptide without spectrin–actin. The total volume was 50–100 μl, and included 50 μM BSA. After 1 h at 37°C, all tubes, up to 10 pairs, were centrifuged together as above. The supernatants and pellets were counted; the amount of bound peptide was typically determined from the difference in peptide concentrations in the supernatants of the sample and control tubes.

Membrane-binding Method

Typically, a small volume of in vitro translated ^{35}S-labeled peptides was mixed with 400 μl of normal membranes. The membranes were obtained by simple hypotonic lysis (10 mM sodium phosphate, 4°C). The mixture of membranes plus peptides was incubated on ice for 20 min (47). To obtain resealed "ghosts" (cells with much reduced hemoglobin), salt was added (100 mM KCl, 1 mM $MgCl_2$), and the membranes were incubated at 37°C for 30–60 min. After resealing, unbound peptide was washed away with isotonic PBS. The washed ghosts were then lysed a second time and rapidly washed in 10 vol of lysis buffer to extract internally free peptide. The pelleted membranes and aliquots from each wash were counted. All centrifugations were done at 15 krpm for 3 min in a 4°C rotor (SS-34; DuPont Instruments, Sorvall Biomedical Division, Wilmington, DE).

FIMD

The micropipette aspiration technique is based upon previous descriptions (13) with equipment differences and an image calibration scheme elaborated elsewhere (12). Details of fluorescent probes and membrane labeling are described elsewhere (12, 18). Labeling of skeletal F-actin was

accomplished with fluorescein or rhodamine phalloidin. Protein 4.1 was purified and labeled by previous methods with FITC (39, 48). Iodoacetim-ido-5-fluorescein (IAF) was conjugated to GST-21.43 and recombinant GST. Polyclonal IgGs to the α-II(44) domain of α-spectrin (S. Marchesi, Yale University, New Haven, CT) were proteolysed to antibody fragments and labeled with FITC. To emulate synthetically a lipid- or glyco-sylphosphatidylinositol (GPI)-linked protein on the red cell's surface, Texas red–conjugated polyclonal IgGs against fluorescein were bound to fluorescein–phosphatidylethanolamine- (FL-PE) labeled red cells.

Calculation of Network Conformation from Density Profiles

For an initial perspective of the analysis, deformation of a linear spring is characterized by one stretch ratio that indicates how the spring is stretched from an initial length L to a final length λL. For an axisymmetric elastic surface deformed to a second axisymmetric surface, the shape change and all geometric quantities are fully described by two stretch ratios, λ_1 and λ_2, which are continuous functions of position along orthogonal lines of curvature on the surface (14, and references therein). As an important application, if the surface density (mass per area) at a material point initially is ρ_o, then the final density, ρ, at that point is determined by how it is stretched: $\rho = \rho_o/\lambda_1\lambda_2$. A relative density can also be defined as $\bar{\rho} = \rho/\rho_o = 1/(\lambda_1\lambda_2)$. The relative density of network components is obtained from FIMD (12) and the network stretches may be calculated by integration (Discher, D., unpublished calculations).

Red Cell Membrane Fragmentation Assays

The strength of membranes in a shearing flow was qualitatively assessed in vitro as described elsewhere (4, 11). Typically, 150–250 μl of membranes was added to an equal volume of peptide. Normal and 4.1-deficient membranes incubated with lysis buffer instead of peptide served as positive and negative controls, respectively.

Results

Interactions with Spectrin–Actin In Vitro Show Minimal Functional Peptides Are the 21.26 and 0.59

The primary goal of this work was to elucidate the mechanism of SAB function in the red cell where the dominant interactions of protein 4.1's SAB occur in a ternary complex formed with F-actin and (limiting) amounts of spectrin at the membrane. The studies presented below therefore focus on this three-component system.

By analyzing the abilities of recombinant SAB peptides to induce gelation (Fig. 2 A) when mixed with F-actin (14 μM) and limiting spectrin (1.8 μM), we first identified peptides with no activity (21.10 and 21.20), weak activity (21.26 and 0.59), and strong activity (21.43 and 21.59) comparable to intact 4.1 (11, 15, also Schischmanoff, P. O., unpublished results). To characterize the mechanism of this gelation, spectrin incorporation into sedimentable, supramolecular assemblies was quantitated by densitometry after electrophoresis (vertical scale, Fig. 2 A). Peptide 21.43 was the most potent in stabilizing spectrin–actin interactions at low concentrations; its activity was again like that of purified 4.1. In comparison, both the 21.26 and 0.59 were between one and two orders of magnitude less active. Peptides shorter than the 21.26 had no effect on spectrin binding to F-actin. Despite the large differences in the activity of these peptides, the onset of gelation was consistently within a relatively narrow concentration range corresponding to 50–65% of spectrin recruitment into ternary complexes (light gray, horizontal band, Fig. 2 A). Thus, the mechanism of network assembly and material strengthening in vitro appears to be based on peptide-dependent sta-
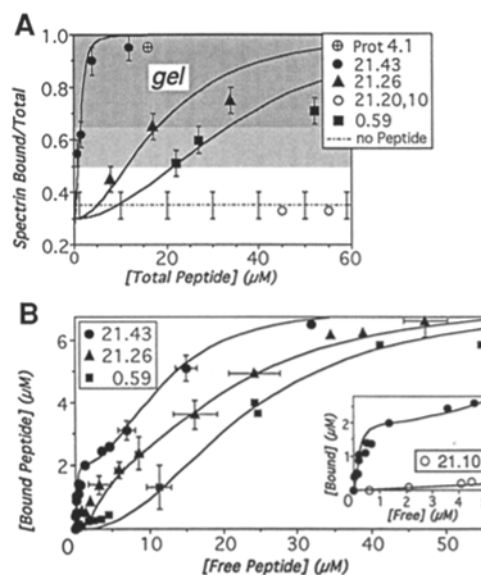
Figure 2. Characterizations of spectrin–actin–SAB peptide complexes as a function of SAB peptide structure and concentration. (A) Viscometry and spectrin cosedimentation assays of peptides mixed with set concentrations of spectrin (1.8 μM) and actin (14 μM). Datapoints indicate both the typical gelation state of the mixtures and the amount of spectrin cosedimenting with F-actin. Data fits are calculated with the ternary complex model (see Results) with parameters listed in Table I. The dark gray zone indicates a consistently obtained gel state for the mixtures. The light gray transition zone covers the range of variation found in the gelation point among a large number of experiments. Peptide 21.20 did not alter mixture viscosity at peptide concentrations up to ~250 μM. The weak spectrin–actin interaction leads to some cosedimentation of spectrin in the absence of any peptide. Both GST fusion peptides and the thrombin-cleaved counterparts gave similar results. (B) ^{35}S-peptide cosedimentation with purified spectrin (2 μM) and actin (7 μM). Error bars indicate the range in data after combining multiple experiments. Data fits are described in the text and summarized in Table I.

bilization of some critical number density of spectrin cross-links between actin filaments.

In related experiments, cosedimentation of ^{35}S-labeled SAB peptides with F-actin (7 μM) and limiting spectrin (2 μM) revealed a two-phase binding process (Fig. 2 B). The 21.43 bound readily into the ternary complex until the spectrin appeared completely complexed with peptide and actin at a stoichiometry of ~1:1 peptide/spectrin (inset, Fig. 2 B). After this first, high affinity, spectrin-dependent phase, there seemed to be a weak, but cooperative, second phase of binding consistent with a binary interaction between peptide and F-actin. In support of this, the second phase of binding saturated at the total F-actin concentration of 7 μM. Decreasing the total F-actin concentration led to a decrease in the magnitude of saturation in this second phase. A weak, and apparently cooperative, interaction between actin and native, full-length 4.1 is consistent with previous reports (2; 36a).

In comparison to the 21.43, the 21.26 and 0.59 showed much less of the first, strong phase of spectrin-dependent binding, but clearly showed a weak, second phase of apparent actin binding. The minimal primary sequence in

common between these two constructs is comprised of the first 26 residues of the constitutive 59-aa domain. These 26 residues are thus implicated as the putative actin binding site in the SAB. Consistent with an important role for actin binding in structural functions like gelation, deletion peptides shorter than the 21.26 did not alter spectrin–actin interactions. Peptide inhibitors of [35]S-21.43 binding included both unlabeled 21.43 and the *Xenopus laevis* SAB, but did not include the small F-actin–binding peptide rhodamine-phalloidin (data not shown).

Ternary Complex Model Includes Cooperativity in Weak F-Actin Binding

A previous analysis of ternary complex assembly (37) included both a spectrin–actin and a spectrin–4.1 association, but did not explicitly include any type of 4.1–actin interaction. The experiments presented in that previous study showed only a single, strong phase of spectrin binding to 10 μM actin in the presence of ~1 μM protein 4.1. This ternary interaction saturated at ~1:1 in 4.1/spectrin, had an apparent binary association constant of ~2 × 10^6 M^{-1}, and yielded a ternary association constant K_3 ~10^{12} M^{-2}. While experiments did not extend beyond this first strong phase of ternary complex formation, the analysis assumed a very weak saturable second phase of 1:1 spectrin/actin interactions with a K_{sa} = 5 × 10^3 M^{-1} estimated from a purely linear binding curve. The ratio of K_3 to K_{sa} gave the thermodynamic contribution of 4.1 to ternary complex stabilization and since this ratio exceeded all prior measures of spectrin–4.1 association constants, the authors concluded that additional binding phenomena may contribute to ternary complex formation.

Based in part on this 1:1:1 stoichiometry in spectrin/actin/4.1 associations, our binding isotherms for the SAB constructs (Fig. 2) also suggest an initial ternary complex phase that uses up the limited spectrin. Our data further show a subsequent binary phase of weak, cooperative binding to F-actin. Cooperativity via an actin lattice is therefore proposed in an approximate ternary complex model (Fig. 3). Linear lattice models involving F-actin have been used before, for example, in matrix-based treatments (21) of cooperativity in troponin–tropomyosin binding to filaments (33). A comparable matrix-based analysis has also been performed on our data (Discher, D., unpublished calculations), but, in an effort to simplify a quantitative presentation, a rudimentary two-term expression is written below for the amount of bound (*B*) SAB peptide as a function of the amount of free (*F*) SAB peptide:

$$B = Sp_o(K_{sp}F)^n/[1+(K_{sp}F)^n] + \{Act_o$$
$$- Sp_o(K_{sp}F)^n/[1+(K_{sp}F)^n]\}(K_{ap}F)^n/[1+(K_{ap}F)^n] \qquad (1)$$

The first term represents spectrin-dependent peptide–actin interactions in the ternary complex: peptide and spectrin are considered to interact while simultaneously bound to different sites on the same actin subunit. This spectrin-dependent component of peptide binding to F-actin is governed by an apparent binary association constant K_{sp} (Fig. 3). The Hill exponent n represents cooperativity, in that whenever peptides are bound on neighboring actin subunits, they interact, perhaps allosterically. The second term rep-
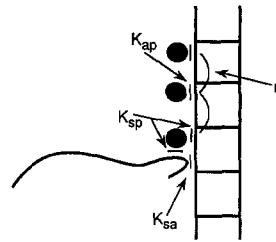

Figure 3. Simplified schematic of protein interaction states in the spectrin–actin–SAB peptide ternary complex. The actin filament is indicated by a ladderlike lattice of subunits that can bind on each actin subunit one SAB peptide, drawn as a black circle, and one spectrin dimer. Cooperativity in binding of SAB peptides occurs through nearest neighbor subunits of an "infinitely long" actin filament.

resents purely peptide–actin interactions; a binary association constant K_{ap} governs this binding.

The four interaction parameters for the data fits in Fig. 2 are tabulated in Table I. For all these fits, n = 2.25. By far the greatest variation among the fits of the 21.43, 21.26, and 0.59 appeared in the spectrin-dependent binding constant K_{sp}. For the 21.43, K_{sp} was on average ~20-fold greater than that for the 21.26, and more than ~50-fold greater than that for the 0.59. These large differences in spectrin-dependent associations offer some explanation for the lack of detectable binary interactions in solution between spectrin and either the 0.59 (11) or the 21.26 (Schischmanoff, P. O., unpublished results). Finally, for an approximate ternary association constant K_3 (M^{-2}) ≈ (2/Sp$_o$)*K_{sa}, the fits listed in Table I for the 21.43 give K_3 ~10^{12} M^{-2} which is in good agreement with previous determinations (38).

SAB Peptide Binding to Normal Membranes Is Spectrin Dependent

Various assays of our SAB peptides' functions inside cells made use of a reversible, lytic incorporation technique. To first elucidate the process of incorporating into a near-normal system, low concentrations (less than or equal to nanomolar) of in vitro translated SAB peptides were loaded into normal cell ghosts during hypotonic lysis. The standard incorporation process (see Materials and Methods) involved a 20-min lysed state on ice during which hemoglobin can leave the cell and peptide can diffuse into the cell through a lytic pore(s) in the membrane (27). Resealed but fairly red ghosts were subsequently washed with PBS to remove radioactive peptide not trapped inside the ghosts (Fig. 4 *A*); the membrane-binding ability of this unincorporated peptide was confirmed in subsequent as-

Table I. Protein 4.1 Peptides in Ternary Complex Formation

	21.43	21.26	0.59
*K_{sp}^{-1} μM	0.75, 0.25	14, 4	26
K_{ap}^{-1} μM	12	22	26
n	2.25	2.25	2.25
‡Sp$_o$ μM	2.0	2.0	2.0
‡Act$_o$ μM	14, 7.25	14, 7.25	14, 7.25

Model fit parameters for ternary complex sedimentation experiments in Fig. 2, *A* and *B*. Association constants are tabulated as their inverse, i.e., dissociation constant.
*Refers to binding of peptide in ternary complex with spectrin–actin.
‡Within 10% of measured concentrations.
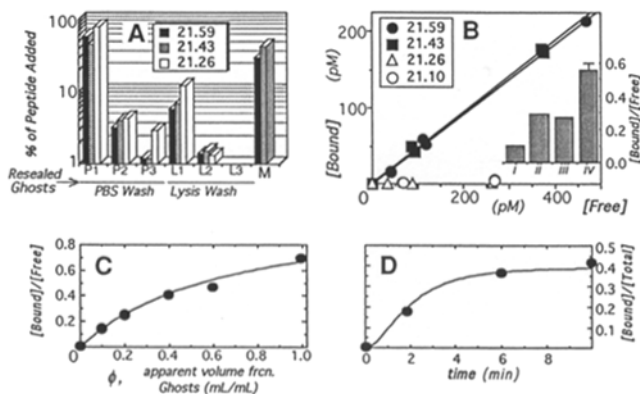
Figure 4. Binding of SAB deletion peptides to normal red cell membranes. (*A*) Analysis of radioactive peptide distribution after incorporation by hypotonic lysis of normal cells and resealing of the ghost membranes (see Materials and Methods). These incorporations were done with 8 μl of each in vitro translated peptide (12–18 nM initial) and 400 μl of membranes. The in vitro synthesis of SAB peptides provided an alternative to bacterial expression and allowed dilute, minimally perturbing tracer studies to be readily performed at the same small scale used in the rest of the work. Resealed ghosts were washed in 10 vol of PBS three times (*P1* to *P3*). The membranes were then relysed in 10 vol (*L1*), centrifuged within 4 min, and washed twice more with lysis buffer (*L2*, *L3*). ^{35}S-peptide content of all the washes and the membrane pellets (*M*) was measured and normalized by the total amount of ^{35}S-peptide added. (*B*) Membrane-bound peptide, as a homogeneous concentration, versus the sum of remaining peptide. The experiments as in *A* were repeated at various initial concentrations of peptide. The inset indicates the slope of the [^{35}S]21.43 binding curves in the presence of various inhibitors: (*i*) GST-21.59 at ~25 μM, (*ii*) GST-XEN at ~25 μM, (*iii*) preincubation with anti-21 aa IgG at ~1 μM, and (*iv*) with no inhibitor present, the average slope ±SD. (*C*) Dependence of 21.59 bound over free on the ghost concentration. Pelleted ghosts were diluted in lysis buffer and treated as in *A*. Model fit of data is described in text. (*D*) Kinetics of 21.59 binding to normal membranes; experiment and model calculation. Experimental determination of binding kinetics followed *A* until 2, 6, or 10 min after the incubation on ice. At each time point, the membranes were diluted 10-fold with lysis buffer, centrifuged for 3 min, and the pellets and supernatants counted. For modeling the incorporation kinetics, it was assumed (19) that 2×10^5 molecules of endogenous 4.1 per cell (2 μM mean intracellular concentration) were in competition with the recombinant 21.59 (at <1 nM) for 2×10^5 skeletal binding sites (2 μM).

say, i.e., the free peptide is not inactive peptide. Parallel studies using fluorescent dextrans (10 kD) and quantitative fluorescence microscopy demonstrated that entrapped concentrations varied by <20% among all cells in a lysed sample. Unbound peptide trapped inside the ghosts by resealing was released by a second lysis with washing before counting the membrane-bound peptide (Fig. 4 *A*).

Recombinant peptides 21.59 and 21.43 bound strongly to red cell membranes with a normal content of endogenous protein 4.1 (Fig. 4, *A* and *B*). The peptide 21.26, functional in ternary complex assays, failed to show significant binding to these membranes even though the 21.26 contains the putative actin-binding site. Consistent with the revelation of a strong spectrin-dependent binding ability,

previous results showed that peptides lacking the 21 aa, including the 0.59, could not bind either spectrin in vitro, or normal membranes in situ (11). Peptides 21.36 and 21.31 were found to bind normal membranes only slightly better than the 21.26 (data not shown), suggesting that these intermediate peptides also interact with spectrin only weakly.

As a further demonstration of membrane-binding specificity, potent inhibitors of the ^{35}S-21.43 were shown to include unlabeled GST-21.59, GST-XEN, an IgG against the 21-aa cassette (*inset*, Fig. 4 *B*), and fluorescently labeled GST-21.43. GST protein alone did not inhibit membrane binding (data not shown). In accordance with the proposed spectrin dependence, as more spectrin was added in the form of ghost membranes (ghost volume fraction φ), membrane binding of the ^{35}S-21.59 also increased (Fig. 4 *C*).

To characterize membrane binding kinetics and verify that an equilibrium could be reached within the 20 min on ice, the time-course for incorporation of the 21.59 was studied systematically. Ghosts lysed for 10 min before the addition of peptide showed the same amount of membrane binding as the typical 20-min reaction on ice. By then adding the 21.59 for preset intervals <10 min and not resealing at all, it was then found that 10 min was necessary to reach equilibrium (Fig. 4 *D*). Since similar binding was obtained in the absence of resealing, the typical 37°C resealing step does not appear to dramatically perturb the 0°C equilibrium. Resealing was highly effective, however, since preincubating ghosts at 37°C for 10 or 30 min before the addition of peptide, reduced membrane binding by >90%.

Spectrin-dependent Competition with Endogenous Protein 4.1

Binding specificity and the correlations with a strong spectrin-dependent association, particularly the lack of membrane interactions of the 21.26, along with the use of compositionally complex normal membranes (wherein $[4.1]_{tot} \approx [Sp]_{tot}$) all suggest that membrane binding is a process involving a competition between the endogenous protein 4.1 and the exogenous SAB for spectrin-dependent binding. Hence, the equilibrium and kinetics of binding (Fig. 4) are analyzed as peptide, P, competing with endogenous 4.1 for binding to skeleton, Sk:

$$P + Sk \leftrightarrow P*Sk \qquad K = k_f/k_r \qquad (2a)$$

$$4.1 + Sk \leftrightarrow 4.1*Sk \qquad K_c = \alpha K \qquad (2b)$$
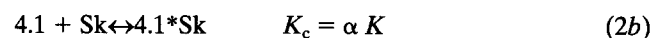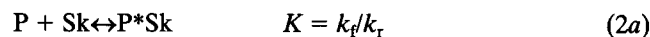
The association constants K and K_c are allowed to differ by an accelerating factor α. We expect the skeletal sites to be spectrin-dependent binding sites. Also, because the spectrin–actin-binding activities of the 21.43 and 4.1 appeared equivalent in vitro, the factor α is intended primarily to capture the effect of protein 4.1's additional interactions with the cytoplasmic domains of both band 3 and the glycophorins (29, 17). These interactions tend to concentrate the endogenous 4.1 to the red cell's periphery in the region of the skeleton, accelerating protein 4.1's interactions with skeletal components.

The fractional saturation of the total sites S_o, $S_o \equiv [Sk]_{tot}$, by the bound peptide, B: $B/S_o = KF/[1 + KF + \alpha KI]$ (21). The total amount of peptide is much smaller than the total concentration of skeletal binding sites, i.e.,

$[P]_{tot} \ll [Sk]_{tot}$. The free 4.1, I, is a small fraction, β, of total 4.1, $I_o \equiv [4.1]tot$. Subscript zeros indicate total cellular concentrations assuming homogeneous solutions of species inside ghosts. The quantity β should be small because, unlike, for example, band 3, most of protein 4.1 is retained in Triton skeletons of membranes (43). If $B \ll I$ and $I \approx \beta[Sk]_{tot}$, then with $\alpha' = \alpha\beta$ and assuming α' is of order one, the binding isotherm becomes: $B/F \approx S_o/[(1/K) + \alpha'S_o]$. The binding data that define F as the sum of external free and internal free (Fig. 4, B and C), give $K = (0.8 \pm 0.1) \times 10^6$ M^{-1}, $\alpha' \sim 1$. Using just the internal free (Fig. 4 A) which includes resealing with salt at 37°C and may therefore give the coarser measure, we get $K = 5 \times 10^6$ M^{-1}, $\alpha' \sim 0.2$.

The order of magnitude of K estimated for SAB interactions with the membrane is comparable to spectrin binding in solution (11). However, since actin is present in the membranes as well, a ternary complex with peptide should form in the membrane so that a more appropriate comparison is to an apparent binary association constant, K_{sp} (M^{-1}), for the first phase of spectrin-limited peptide binding to actin in a ternary-complex. As in the ternary-complex analysis, $K_{sp} \approx (S_o/2)K_3$; hence a $K_{sp} \sim 10^6$ M^{-1} is estimated from $K_3 \approx 10^{12}$ M^{-2} and $S_o \approx 2$ μM.

The incorporation kinetics data were fit (Fig. 4 D) by the solution of two coupled ordinary differential equations based on the competitive binding model (Eqs. 2a and 2b) and using $K = 0.9 \times 10^6$ M^{-1}, $\alpha \sim 5$, $\beta = 0.04$ to 0.2, and $k_f = 0.5 \times 10^4$ M^{-1}s^{-1}. Thus, endogenous protein 4.1 has a slight kinetic advantage (fivefold) in binding to the skeleton from its vantage point on integral membrane proteins.

Membrane Localization of Fluorescent SAB Peptide In Situ

As a means of explicitly verifying membrane localization and proper integration into network structure, fluorescently labeled molecules in resealed ghosts were imaged after aspirating a ghost into a glass micropipette (Fig. 5). The phospholipid analogue FL-PE readily intercalates into the bilayer and gives a definitive edge-brightness to the image of the sphere outside the pipette (Fig. 5 B). Fluorescein-labeled antibody fragment against spectrin (Fig. 5 C) and fluorescein or rhodamine-phalloidin (Fig. 5 D) label only the inner surface of membranes. The phalloidin presumably binds to F-actin ($\sim 4 \times 10^5$ sites per cell [19]). Both FITC-4.1 (Fig. 5 E) and IAF-GST-21.43 (Fig. 5 F) showed moderate edge brightness inside 4.1-deficient ghosts ($\sim 2 \times 10^5$ skeletal sites per cell [19, 26]) as expected from the radiometric binding analyses. IAF-GST (Fig. 5 G), albumin, and dextran controls appeared only diffusely distributed in the cytoplasm at all concentrations. Antifluorescein IgG bound readily to FL-PE–labeled cells (Fig. 5 G). A rhodamine-labeled mAb fragment recognizing GPI-anchored CD-59 ($\sim 4 \times 10^4$ sites per cell [22]) labeled membranes only dimly (12) even near saturation in binding.

Conventional microscopy was used for most of the imaging since it provides a sensitivity advantage, but optical sectioning (Fig. 6 A, inset) was also used to clearly verify edge enrichment. Quantitatively, for a sphered ghost cytoplasmic vol of ~ 150 μm^3 filled by unbound label and a
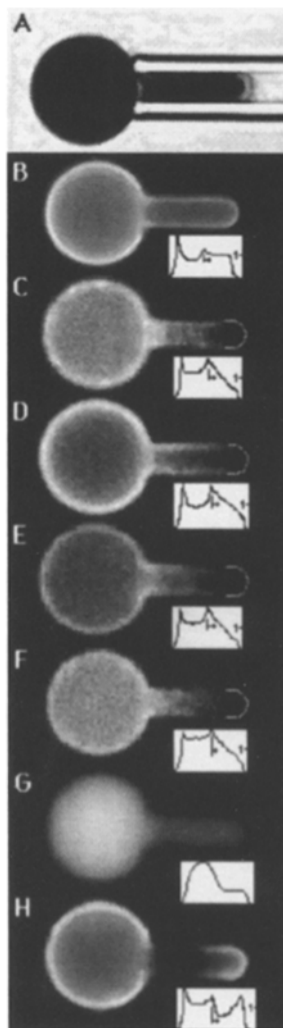
Figure 5. Images of fluorescently labeled membrane components on red cells or resealed ghosts in the aspirated configuration. (A) Bright-field image of an osmotically pressurized red cell after aspiration into a micropipette (see Materials and Methods; 12). (B) Typical distribution of the lipid bilayer as labeled with FL-PE. Inset figure shows the integrated intensity profile obtained by summing pixel intensities across the diameter of the aspirated projection. The pipette entrance is indicated with an arrow. The largest peak in the profile arises from the portion of the sphere's image diametrically opposite the pipette entrance. Note the uniformity of response along the projection. (C, D, and E) Typical deformation response of the red cell skeleton as revealed by spectrin-, actin-, or 4.1-labeled red cell ghosts, respectively. Probes were incorporated by reversible hemolysis. Anti-spectrin antibody fragments and rhodamine-phalloidin were used to label spectrin and F-actin, respectively. FITC-4.1 was incorporated in 4.1-deficient red cell ghosts. Inset figures show the integrated intensity profiles; the intensity at the tip is well above zero. Note the strong decrease from the pipette entrance to the tip of the projection which contrasts with the lipid profile. Also note the relative uniformity of signal along the rim of the sphere's image. (F) A similar distribution in the projection of 4.1-deficient red cells containing bacterially expressed GST-21.43 labeled with IAF. The dye/protein ratio was 1:1.6 and the IAF-labeled peptide could inhibit binding of radioactive 21.59 to normal membranes. (G) Incorporation of fluoresceinated GST as a control for F. No membrane association and no graded response in the aspirated projection were observed in the range of 1 to 15 μM. (H) Distribution of lipid-linked IgG. Anti-fluorescein antibodies were bound to FL-PE–labeled red cells. Antibody fragment–labeled, GPI-anchored CD-59 gave a similar response of protein concentrated at the tip of the projection (12).

range in skeletal thickness between 5 and 100 nm (estimated from either actin monomer dimensions or spectrin dimer contour length; 5) binding sites at the membrane would be enriched relative to the cellular concentration by between 200- and 12-fold, respectively. For protein 4.1, these numbers imply that its apparent concentration at the membrane ranges between 36 and 600 μM, substantially higher than its mean cellular concentration of 3 μM. As further evidence, edge brightness with rhodamine-phalloidin was measured as a function of added phalloidin (Fig. 6 A); a fit of the phalloidin-binding data with a simple bimolecular model indicated a high-affinity membrane association constant that was within a factor of 7 of in vitro mea-
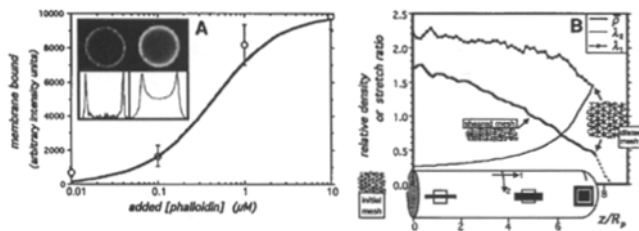
Figure 6. (*A*) Specificity of rhodamine-phalloidin labeling of a normal ghost membrane. Left inset image is a rhodamine-phalloidin–labeled ghost imaged with a confocal microscope; right image is taken with a conventional fluorescence microscope. The curve indicates edge intensity of images using conventional microscopy and measured as a function of total phalloidin added. Rhodamine-phalloidin was serially diluted in lysis buffer, after measuring the highest concentration using a dye/phalloidin ratio of 1:1 and a peak absorptivity of 76,000 $M^{-1}cm^{-1}$. The fitted curve used 2 × 10^{-7} M for the concentration of F-actin binding sites as calculated from 4 × 10^5 actin molecules per membrane (19) and the volume of cells lysed. The apparent association constant is 0.33 × 10^7 M^{-1} which is slightly weaker than in vitro assays. Average ±SD are shown for at least nine ghosts labeled at each concentration. (*B*) Localized network stretching conformations and SAB peptide integration. Plot of a typical network density profile, $\bar{\rho}$, on an aspirated membrane projection along with calculated stretch ratios: axial stretch, λ_1, and circumferential stretch, λ_2 (see Materials and Methods). The abscissa is in the shape of the aspirated projection, and shows the axial distance z scaled by the pipette radius R_p. To the left of the projection is illustrated a square piece of the cytoskeletal meshwork before deformation. This meshwork is dilated at the tip of the projection, and about halfway down the cylinder the meshwork is in a rectangular state of pure shear. The principal directions of stretch and the deformation of an initial square are also sketched on the projection.

surements for phalloidin binding to F-actin. These coarse calculations together with the confocal image (Fig. 6 *A, inset*) provide more explicit illustrations of the membrane-concentrating effect and demonstrate that physiological concentrations can be much higher than the micromolar range.

In Situ Integration into the Solidlike Cytoskeletal Network

In cells other than erythrocytes, actin-binding proteins localize to stress fibers, focal contacts, and a number of other structures (e.g., 34). If one were to deform reversibly such cells and redistribute the structures, one would still expect to see a colocalization of the actin and actin-binding proteins to the same redistributed structures. In the aspirated images of Fig. 5 then, specificity of localization and structural connectivity are indicated by the fluorescence patterns obtained after deforming the uniformly labeled red cell into the micropipette (12). In short, FL-PE shows that the lipid bilayer convects like a fluid sheet to cover uniformly (Fig. 5 *B*) a strong gradient in density of the underlying skeleton as labeled with either antispectrin, rhodamine–phalloidin, FITC-4.1, or IAF-GST-21.43 (Fig. 5, *C*, *D*, *E*, and *F*, respectively). Formation of this density gradient is much like the very tangible process of pushing a finger into the palm of a rubber glove: looking towards the extreme tip of the finger, one sees that the material be-

comes progressively more dilated. Important in contrast, is the finding that lipid-linked proteins, both lipid-bound antibody (Fig. 5 *H*) and GPI-anchored protein CD-59 (12), which presumably have no means for connection to the underlying skeleton, give a response in deformation nearly opposite to the network probes (12, for clarification).

Quantitative "fingerprints" of these component distributions are given by the intensity sections along the projections shown in small insets below each cell (Fig. 5, *insets*). For lipid probe, the intensity is nearly uniform, but for spectrin, actin, 4.1, and recombinant SAB peptide, a strong gradient in density appears. Particularly note that these insets show the network density is nonvanishing at the tip of the projection. This gradient is stable (up to 30 min) and reversible upon release from aspiration, indicating a solidlike skeletal network and consistent with a resilient and durable membrane. The two-dimensional nature of the network permits calculation (see Materials and Methods) of how an initially small square of cytoskeletal meshwork can, depending on its location, be transformed to various rectangular conformations down the length of the projection (Fig. 6 *B*). At the very tip or cap of the projection, the initially square bit of meshwork is simply dilated in the deformation. Toward the pipette entrance, the material is highly stretched in the axial direction, but compressed in the lateral direction; this conformational state is one of extensive shearing and is a sustainable state for a solidlike but not a labile, fluidlike network. The fact that the SAB peptide gives the same apparent density field along the projection as the native skeletal components, explicitly shows integration of the peptide into the same elastic network structure whether this structure is sheared, dilated, or compressed reversibly. This suggests that both the SAB peptide and protein 4.1 should have similar effects on network integrity or strength.

Red Cell Membrane Strength Is Determined by SAB Peptides' Ability to Stabilize Spectrin Cross-links of Actin In Situ

Red cells deficient in protein 4.1 possess membranes that are more fragmentable than normal membranes (46, 51). However, both purified, exogenous 4.1 (47) and recombinant GST-21.59 (11) can, at approximately micromolar cellular concentrations, increase membrane strength to normal. To test this crucial aspect of in situ cellular function of our SAB constructs, mutant red cells with deficiencies in protein 4.1 were lysed in the presence of each peptide. After resealing and suspending the ghosts in a viscous dextran, each sample was subjected to a membrane-fragmentation assay.

Initially, the deformation response for all the samples is about the same value (Fig. 7), indicating that all ghosts start as comparably stretched ellipsoids. After a very short interval of sustained deformation, however, the 4.1-deficient membranes (~40% deficiency) show a transition to steady fragmentation as indicated by the decay in the deformation index. Normal membranes fragment much later. Addition of the peptide 21.20 to the 4.1-deficient membranes did not alter the membrane fragmentation process (Fig. 7 *A*). The 21.43, in contrast, was able to strengthen the 4.1-deficient membranes to a level comparable to nor-
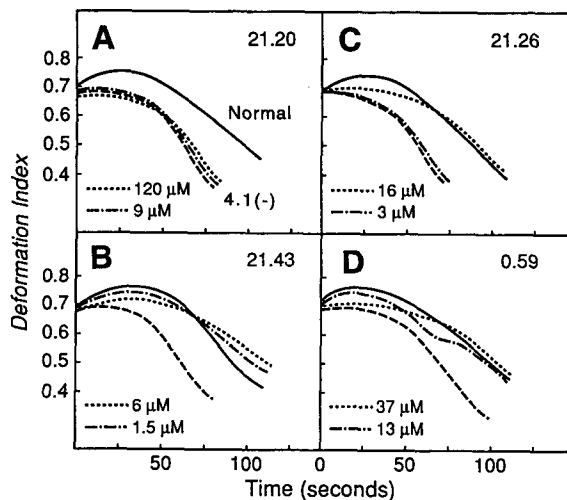
Figure 7. Membranes can be strengthened by peptides 21.43, 21.26, and 0.59, but not 21.20 at high concentrations. Thrombin-cleaved, ^{35}S-labeled peptides were added to ghosts prepared from partially (~40%) 4.1-deficient red cells. Peptide added equals the amount of total peptide divided by the volume after addition to membranes. The relative strength of the resealed membranes was assessed by membrane fragmentation under fluid shear and is plotted as a time-dependent decline in deformation index. Responses of normal (*solid line*) and 4.1(−) membranes (*large dashed line*) defined the range of membrane strengthening effect for each construct. (*A*) Peptide 21.20, even at very high concentrations, did not alter the fragmentation rate. (*B*) Peptide 21.43 restored membrane strength at as low as 1.5 μM, consistent with published results for either purified protein 4.1 or GST-21.59, while (*C*) increasing the concentration of 21.26 resulted in a decreased rate of fragmentation, hence increased membrane strength. (*D*) Entrapment of 0.59 at 37 μM and, to a lesser extent, at 13 μM showed a positive effect.

mal (Fig. 7 *B*), and, as with the 21.59 (11; data not shown), only micromolar (~1.5 μM) concentrations of the 21.43 were necessary. Equivalent strengthening with the peptides 21.26 and 0.59 (Fig. 7, *C* and *D*, respectively) required much higher peptide concentrations (>15 μM). A measure of specificity for these effects is manifest in a 21.20 concentration of ~120 μM having no effect on membrane strength (Fig. 7 *A*). GST-21.10, GST-21.20, and GST in membranes with a full, 100% 4.1 deficiency (data not shown) also showed no effect. However, *X. laevis* SAB, as might be expected from the remarkable homology with human SAB, considerably strengthened the 4.1-deficient human red cells (Winardi, R., unpublished data).

For a quantitative approach to the incorporation chemistry, we used ^{35}S-labeled, thrombin-cleaved peptides in the fragmentation assays. Measurements of the entrapped peptide concentrations showed that the concentration of the inactive peptide 21.20 inside ghosts was linear over the full range of added peptide, extending to ~50 μM entrapped. In contrast, the amounts of 21.43, 21.26, and 0.59 entrapped at a given concentration of added peptide were consistently higher than the 21.20, and appeared as an additional, specific membrane-binding component. The amount of specific binding (Fig. 8 *A*) was therefore obtained by subtracting the baseline amount of 21.20 physically entrapped by resealing. In addition, for the 21.43 at two con-
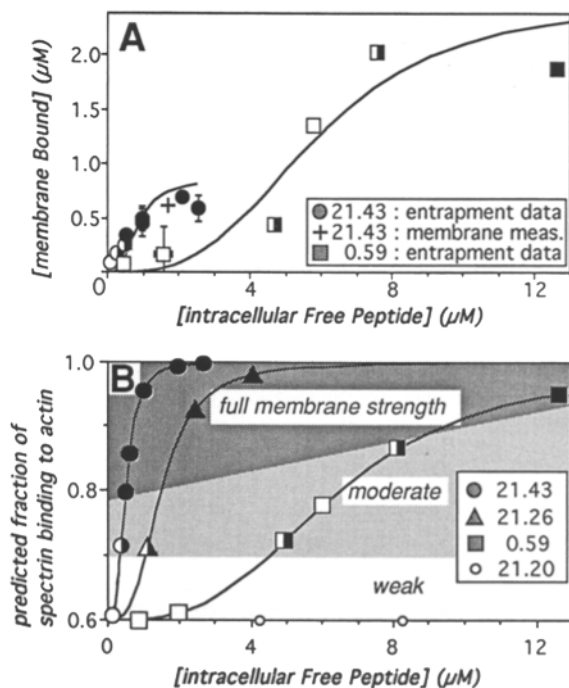
Figure 8. Binding of active peptides to 4.1-deficient ghost membranes and predicted extent of in situ spectrin–actin interactions. ^{35}S-labeled peptides were entrapped inside the ghosts and used in the fragmentation assays of Fig. 7 *B*. (*A*) Specific binding of labeled 21.43, and 0.59, respectively, as calculated by subtracting the nonspecific, physical entrapment of 21.20. For the 21.43, two data points indicated by + are measured after lysis as in Fig. 4; one + lies on the curve at ~0.4 μM. Data points in each panel are solid if the strengthening effect was nearly full effective; half-shaded points correspond to a partial effect on membrane strength. Open points indicate no clear effect on membrane strength. Curves are calculated with the ternary complex model (see Results) and the parameters given in Table II. Intracellular concentrations are with respect to cell volume; they do not reflect the membrane localization effect. (*B*) For each peptide, the predicted fraction of spectrin bound to actin is illustrated against a background shading scheme representative of the effect on membrane strength. The curves are generated from the fits of Fig. 8 *A*. No shading indicates no effect on membrane strength. Light gray indicates partial effect. Darker gray indicates nearly full effect.

centrations, the amount of membrane-bound peptide after a second lysis was directly measured (as per Fig. 4 *A*), and was found to coincide with the calculation based on subtraction of the 21.20 baseline. When the ternary complex model was fit through the membrane-binding data (Fig. 8 *A*), we used a value for available spectrin (0.8 μM = 40% of 2 μM) consistent with an ~40% (32) deficiency in endogenous protein 4.1 (normally 2 μM). The actin available for binding used in fitting the results (2.4 μM; Table II) appears to be slightly less than an estimate (2.9 μM) based on the total actin content (4.1 μM) minus the endogenous 4.1 (60% of 2 μM). Importantly, the trends in spectrin-dependent binding constants obtained in vitro (Table I) are substantially replicated in the fits of binding to membrane structures in situ (Table II). Competition with endogenous 4.1 has been ignored in this membrane-binding analysis, since such competition is likely to have an effect only at high 21.43 concentrations after the 40% of skeletal

Table II. Interaction of Protein 4.1 Peptides with the Membrane

	21.43	21.26	0.59
K_{sp}^{-1} μM	0.75	1.5	6.5
K_{ap}^{-1} μM	8	2.9	6.5
n	3	3	3
*Sp$_o$ μM	0.8	0.8	0.8
*Act$_o$ μM	2.4	2.4	2.4

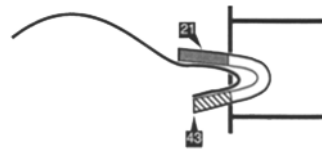Model fit parameters for binding of peptides to membranes (Fig. 8 *A*) used in fragmentation assay.
*Within 15% of estimated concentrations.

Figure 9. Structural model of the SAB domain's protein interactions. The middle, unshaded domain represents the proposed actin-binding site of 26 residues in the constitutively expressed 59-aa domain. Strong spectrin binding requires both the stippled 21-aa cassette and the striped COOH-terminus ending near residue 43 of the 59-aa domain.

sites left unoccupied by 4.1 become largely filled by the 21.43.

Full membrane-strengthening effect (Fig. 8 *A*, *solid points*) by the 21.43 occurs with much lower binding to the membrane (>0.3 μM) than required for the 0.59 (~2 μM). The underlying mechanism that gives rise to this approximately sevenfold difference in effectiveness is significantly clarified, however, by calculating for each SAB construct the peptide-facilitated increase in spectrin–actin associations in the membrane. This spectrin-dependent phase of the binding of each peptide, the first term in Eq. 1, is plotted as the predicted fraction of membrane spectrin that binds to actin. A background shading scheme also illustrates the effect on membrane strength (Fig. 8 *B*). As found in vitro (Fig. 2 *B*), spectrin–actin stabilization is very closely associated with material strengthening.

Discussion

COOH-terminal deletion constructs and an NH$_2$-terminal isoform of protein 4.1's SAB domain have been assayed for their ability to enter into ternary associations with spectrin–actin in vitro and also to specifically bind, integrate into, and mechanically strengthen red cell membranes in situ. Highly efficient, membrane-strengthening interactions involving both spectrin and actin require both the NH$_2$-terminal 21 aa, and also the 43 residues of the constitutive 59-aa domain. However, a reduced yet adequate, membrane-strengthening activity arises from either the 21 aa together with the first ~26 residues of the 59 aa or just the 59 aa alone. Combined with similar findings in ternary complex formation in vitro, a simplistic structural model of SAB function emerges (Fig. 9): two sites for spectrin interaction flank the ~26 residue actin-binding site. Exactly half of the residues of the putative actin-binding site are charged, consistent with localization to the protein surface. This sequence also contains Lys[447] which, through deletion of this conserved 20th of 26 residues, has recently been implicated in both defective red cell membranes and an inability to bind spectrin–actin (30). The two putative spectrin-binding sites are largely conserved among species, consistent with our results for *X. laevis* 21.59 (Fig. 4 *B*). Structural artifacts arising from peptide construction could contribute to the results, but preliminary CD spectra suggest that small if any changes in global peptide conformation result from our deletions in primary structure (Schischmanoff, P. O., unpublished data). In further support of two spectrin sites, a tyrosine kinase phosphorylates near the middle of the 21 aa (45) while a serine

kinase phosphorylates at the 40th residue of the 59 aa (23); both phosphoadducts of the SAB have substantially reduced spectrin–actin-binding activity (28, 45). Thus, in addition to the very strong genetic modulation of activity provided by splicing in or out the alternative NH$_2$-terminal exon, the split in the spectrin-binding interaction establishes two physiological pathways for strong modulation via posttranslational modification.

Because the constitutive 59-aa domain on its own is found functional, albeit weakly, in both gelation and membrane-strengthening assays, expression of the alternatively spliced 21 aa may be interpreted as a biologically efficient (42), rather than physically necessary means of achieving the red cell membrane's required strength. It should be emphasized that the mean intracellular concentration of 0.59 sufficient for fully normal strengthening (~12 μM, Fig. 8) is substantially below the minimum estimate of protein 4.1 concentration at the membrane (>36 μM).

After controlled, reversible aspiration of ghosts, spectrin, actin, 4.1, and the recombinant 21.43 appeared to have moved collectively as an integrated structural unit. Fragmentation of 4.1-deficient red cell membranes under high fluid shear was subsequently shown to be modulated by the SAB peptides' abilities to bind spectrin–actin. The rapid, fluid-forced fragmentation of the red cell membrane seems likely to be a process of catastrophic failure at the weakest point in the structure. In the absence of protein 4.1, the membrane's weak point would appear to be the bare spectrin–actin interaction. Addition of enough of a recombinant SAB peptide, even an inefficient stabilizer like the 0.59, ultimately shifts the membrane's weak point to another set of strength limiting interactions. Below this strength limit, concomitant increases in spectrin–actin stabilization and material strength, either membrane strength (Fig. 8 *B*) or gel strength (Fig. 2 *A*), appear roughly peptide independent. This suggests that, for all the functional SAB peptides, it is primarily the stabilization of spectrin cross-links of F-actin that solidifies and strengthens the structure.

Like protein 4.1, the spectrin–actin-stabilizing phosphoprotein adducin seems to bind F-actin cooperatively (35). Adducin's binary interaction with actin can cooperatively drive spectrin into a spectrin–actin–adducin ternary complex, similar perhaps to the SAB peptides 21.26 and 0.59, which interact with spectrin only weakly (Fig. 2 *A*). β-adducin is also alternatively spliced, and occurs in a number of tissues as an isoform lacking portions of the spectrin–actin binding COOH-terminus (Gilligan, D. M., and V. Bennett. 1994. *Mol. Biol. Cell.* 5:421a; Hughes, C. A., and V. Bennett. 1994. *Mol. Biol. Cell.* 5:421a).

The present data reinforce the finding (11) that protein

4.1's role in membrane strength, as assessed by the fluid shear–fragmentation assay, is essentially determined by its SAB interactions, independent of further associations of protein 4.1 with glycophorins, p55, band 3, or phosphatidylserine. A role for glycophorin C as a site for linking the bilayer and network was suggested by studies showing glycophorin C–deficient red cells are more easily fragmented in fluid shear than normal membranes (43). However, additional studies of the glycophorin C deficiency have noted a coexisting deficiency in protein 4.1 (1), and we have recently found that addition of either purified protein 4.1 or just an SAB peptide to red cells completely deficient in glycophorin C strengthened these membranes to normal (Discher, D., D. Knowles, S. McGee, M. Parra, J. Conboy, and N. Mohandas. 1993. *Mol. Biol. Cell.* 4:169a). Interestingly, like protein 4.1, red cell adducin also seems to interact with an integral membrane protein (Sinard, J. H., G. W. Stewart, A. C. Argent, and J. S. Morrow. 1994. *Mol. Biol. Cell.* 5:421a). The present results tentatively suggest, however, that an adducin-mediated linkage between the network and bilayer is not critical to the membrane's resistance against fluid shear fragmentation.

A membrane compartmentalization role for the interactions protein 4.1 has with bilayer structures was postulated in our initial report of the membrane-strengthening effect of the SAB (11). Interactions at the membrane clearly have a concentrating effect (e.g., Fig. 6 *A*, *inset*). For protein 4.1, peripheral interactions with bilayer structures would tend to accelerate its interactions with network spectrin and actin. Quantitative evidence for this hypothesis was provided, to a limited extent, by the competitive binding of SAB to normal membranes: multifunctional 4.1 appears to have a fivefold kinetic advantage in competition for network binding. The net result of this mechanism for membrane localization may be an evolved effort to economize with a fixed and minimal amount of protein. Splicing in the 21-aa cassette has a similar effect as it tremendously increases SAB activity and thereby reduces the amount of free protein. Both of these mechanisms for the enhanced binding of 4.1 to spectrin–actin in situ thus act to minimize the total amount of protein needed for network stabilization. The studies presented here on the mechanochemistry of protein 4.1's SAB domain therefore support the idea that, besides the possibilities of contributing directly to cell mechanical properties, multiplicity in structural protein interactions can play an important role in cell protein economics.

References

1. Alloisio, N., N. D. Venezia, A. Rana, K. Andrabi, P. Texier, J.-P. Cartron, J. Delaunay, and A. H. Chisti. 1993. Evidence that red blood cell protein p55 may participate in the skeleton–membrane linkage that involves protein 4.1 and glycophorin C. *Blood.* 82:1323–1327.
2. Becker, P. S., M. A. Schwartz, J. S. Morrow, and S. E. Lux. 1990. Radiolabel-transfer cross-linking demonstrates that protein 4.1 binds to the N-terminal region of beta-spectrin and to actin in binary interactions. *Eur. J. Biochem.* 193:827–836.
3. Bennett, V. 1985. The membrane skeleton of human erythrocytes and its implication for more complex cells. *Annu. Rev. Biochem.* 54:273–304.
4. Bessis, M., and N. Mohandas. 1975. A diffractometric method for the measurement of cellular deformability. *Blood Cells (NY).* 1:307–313.
5. Byers, T. J., and D. Branton. 1985. Visualization of the protein associations in the erythrocyte membrane skeleton. *Proc. Natl. Acad. Sci. USA.* 82:6151–6157.
6. Cantor, C. R., and P. R. Schimmel. 1980. Biophysical Chemistry. W. H. Freeman and Co. Publisher. New York. 375–379.
7. Cohen, C. M., and C. Korsgren. 1980. Band 4.1 causes spectrin-actin gels to become thixotropic. *Biochem. Biophys. Res. Commun.* 97:1429–1435.
8. Conboy, J. G., J. Chan, N. Mohandas, and Y. W. Kan. 1988. Multiple protein 4.1 isoforms produced by alternative splicing in human erythroid cells. *Proc. Natl. Acad. Sci. USA.* 85:9062–9065.
9. Cooper, J. A., and T. D. Pollard. 1982. Methods to measure actin polymerization. *Methods Enzymol.* 85:182–233.
10. Correas, I., T. L. Leto, D. W. Speicher, and V. T. Marchesi. 1986. Identification of the functional site of erythroid protein 4.1 involved in spectrin–actin associations. *J. Biol. Chem.* 261:3310–3315.
11. Discher, D., M. Parra, J. G. Conboy, and N. Mohandas. 1993. Mechanochemistry of the alternatively spliced spectrin–actin binding domain in membrane skeletal protein 4.1. *J. Biol. Chem.* 267:7186–7195.
12. Discher, D. E., N. Mohandas, and E. A. Evans. 1994. Molecular maps of red cell deformation: hidden elasticity and in situ connectivity. *Science (Wash. DC).* 266:1032–1035.
13. Evans, E. A. 1989. Structure and deformation properties of red blood cells: concepts and quantitative methods. *Methods Enzymol.* 173:3–35.
14. Evans, E. A., and R. Skalak. 1980. Mechanics and Thermodynamics of Biomembranes. CRC Publications, Grand Rapids, MI. 254 pp.
15. Fowler, V., and L. Taylor. 1980. Spectrin plus band 4.1 cross-link actin—regulation by micromolar calcium. *J. Cell Biol.* 85:361–376.
16. Gardner, K., and V. Bennett. 1989. Recently identified erythrocyte membrane-skeletal proteins and interactions: implications for structure and function. *In* Red Blood Cell Membranes. P. Agre and J. H. C. Parker, editors. Marcel Dekker, New York. 1–29.
17. Gascard, P., and C. M. Cohen. 1994. Absence of high-affinity band 4.1 binding sites from membranes of glycophorin C- and D-deficient erythrocytes. *Blood.* 83:1102–1108.
18. Golan, D. E., C. S. Brown, C. M. L. Cianci, S. T. Furlong, and J. P. Caulfield. 1986. Schistosomula of *Schistosoma mansoni* use lysophosphatidylcholine to lyse adherent human red blood cells and immobilize red cell membrane components. *J. Cell Biol.* 103:819–828.
19. Goodman, S. R., K. E. Krebs, C. F. Whitfield, B. M. Riederer, and I. S. Zagon. 1988. Spectrin and related molecules. *Crit. Rev. Biochem.* 23:171–234.
20. Guan, K.-L., and J. E. Dixon. 1991. Eukaryotic proteins expressed in *Escherichia coli*: an improved thrombin cleavage and purification procedure of fusion proteins with glutathione S-transferase. *Anal. Biochem.* 192:262–267.
21. Hill, T. L. 1985. Cooperativity Theory in Biochemistry—Steady-State and Equilibrium Systems. Springer-Verlag New York, Inc., New York. 459 pp.
22. Holguin, M. H., and C. J. Parker. 1992. Membrane inhibitor of reactive lysis. *In* Current Topics in Microbiology and Immunology C. J. Parker, editor. 178:61–86.
23. Horne, W. C., W. C. Prinz, and E. K.-Y. Tang. 1990. Identification of two cAMP-dependent phosphorylation sites on erythrocyte protein 4.1. *Biochim. Biophys. Acta.* 1055:87–92.
24. Horne, W. C., S.-C. Huang, P. S. Becker, T. K. Tang, and E. J. Benz, Jr. 1993. Tissue-specific alternative splicing of protein 4.1 inserts an exon necessary for formation of the ternary complex with erythrocyte spectrin and F-actin. *Blood.* 82:2558–2563.
25. Huang, J.-P., C.-J. Tang, G.-H. Kou, V. T. Marchesi, E. J. Benz, and T. K. Tang. 1993. Genomic structure of the locus encoding protein 4.1—structural basis for complex combinational patterns of tissue-specific alternative RNA splicing. *J. Biol. Chem.* 268:3758–3766.
26. Kishino, A., and T. Yanagida. 1988. Force measurements by micromanipulation of a single actin filament by glass needles. *Nature (Lond.).* 334:74–76.
27. Lieber, M. R., and T. L. Steck. 1982. A description of the holes in human erythrocyte membrane ghosts. *J. Biol. Chem.* 257:11651–11659.
28. Ling, E., Y. N. Danilov, and C. M. Cohen. 1988. Modulation of red cell band 4.1 function by cAMP-dependent kinase and protein kinase C phosphorylation. *J. Biol. Chem.* 263:2209–2216.
29. Lombardo, C. R., B. M. Willardson, and P. S. Low. 1993. Localization of the protein 4.1-binding site on the cytoplasmic domain of erythrocyte

membrane band 3. *J. Biol. Chem.* 267:9540–9546.

30. Lorenzo, F., N. D. Venezia, L. Morlé, F. Baklouti, N. Alloisio, M.-T. Du-cluzeau, L. Roda, P. Lefrancois, and J. Delaunay. 1994. Protein 4.1 deficiency associated with an altered binding to the spectrin–actin complex of the red cell membrane skeleton. *J. Clin. Invest.* 94:1651–1656.

31. Mach, H., C. R. Middaugh, and R. V. Lewis. 1992. Statistical determination of the average values of the extinction coefficients of tryptophan and tyrosine in native proteins. *Anal. Biochem.* 200:74–80.

32. McGuire, M., B. L. Smith, and P. Agre. 1988. Distinct variants of erythrocyte protein 4.1 inherited in linkage with elliptocytosis and Rh type in three white families. *Blood.* 72:287–293.

33. Mehegan, J. P., and L. S. Tobacman. 1991. Cooperative interactions between troponin molecules bound to the cardiac thin filament. *J. Biol. Chem.* 266:966–972.

34. Menkel, A. R., M. Kroemker, P. Bubeck, M. Ronsiek, G. Nikolai, and B. M. Jockusch. 1994. Characterization of an F-actin–binding domain in the cytoskeletal protein vinculin. *J. Cell Biol.* 126:1231–1240.

35. Mische, S. M., M. S. Mooseker, and J. S. Morrow. 1987. Erythrocyte addcin: a calmodulin-regulated actin-bundling protein that stimulates spectrin–actin binding. *J. Cell Biol.* 105:2837–2845.

36. Mohandas, N., and E. A. Evans. 1994. Mechanical properties of the red cell membrane in relation to molecular structure and genetic defects. *Annu. Rev. Biophys. Biomol. Struct.* 23:787–818.

36a. Morris, M. B., and S. E. Lux. 1995. Characterization of the binary interaction between 4.1 and actin. *Eur. J. Biochem.* In press.

37. Ohanian, V., L. C. Wolfe, K. M. John, J. C. Pinder, S. E. Lux, and W. B. Gratzer. 1984. Analysis of the ternary interaction of the red cell membrane skeletal proteins spectrin, actin, and 4.1. *Biochemistry.* 23:4416–4420.

38. Pardee, J. D., and J. A. Spudich. 1982. Methods to measure actin polymerization. *Methods Enzymol.* 85:164–181.

39. Podgorski, A., and D. Elbaum. 1985. Properties of red cell membrane proteins: mechanism of spectrin and band 4.1 interaction. *Biochemistry.* 24:7871–7876.

40. Ralston, G. B. 1976. Physico-chemical characterization of the spectrin tetramer from bovine erythrocyte membranes. *Biochim. Biophys. Acta.* 455:163–172.

41. Reid, M. E., J. A. Chasis, and N. Mohandas. 1987. Identification of a functional role for human erythrocyte sialoglycoproteins beta and gamma. *Blood.* 69:1068–1072.

42. Seidel, H. M., D. L. Pompliano, and J. R. Knowles. 1992. Exons as microgenes? *Science (Wash. DC).* 257:11489–11490.

43. Sheetz, M. P. The bilayer and shell model of the erythrocyte membrane. *In* Erythrocyte Mechanics and Blood Flow. G. R. Cokelet, H. J. Meiselman, and D. E. Brooks, editors. Alan R. Liss, Inc., New York. 1–13.

44. Shields, M., P. LaCelle, R. E. Waugh, M. Scholz, R. Peters, and H. Passow. 1987. Effects of intracellular Ca^{2+} and proteolytic digestion of the membrane skeleton on the mechanical properties of the red blood cell membrane. *Biochim. Biophys. Acta.* 905:181–194.

45. Subrahmanyam, G., P. J. Bertics, and R. A. Anderson. 1991. Phosphorylation of protein 4.1 on tyrosine-418 modulates its function in vitro. *Proc. Natl. Acad. Sci. USA.* 88:5222–5226.

46. Tchernia, G., N. Mohandas, and S. B. Shohet. 1981. Deficiency of skeletal membrane protein band 4.1 in homozygous hereditary elliptocytosis. *J. Clin. Invest.* 68:454–460.

47. Takakuwa, Y., G. Tchernia, M. Rossi, M. Benabadji, and N. Mohandas. 1986. Restoration of normal membrane stability to unstable protein 4.1–deficient erythrocyte membranes by incorporation of purified protein 4.1. *J. Clin. Invest.* 78:80–85.

48. Tyler, J. M., W. R. Hargreaves, and D. Branton. 1979. Purification of two spectrin-binding proteins. Biochemical and electron microscopic evidence for site-specific reassociation between spectrin and band 2.1 and 4.1. *Proc. Natl. Acad. Sci. USA.* 76:5192–5196.

49. Ungewickell, E., P. M. Bennet, R. Calvert, V. Ohanian, and W. B. Gratzer. 1979. In vitro formation of a complex between cytoskeletal proteins of the human erythrocyte. *Nature (Lond.).* 280:811–814.

50. Ungewickell, E., and W. Gratzer. 1978. Self-association of human spectrin: a thermodynamic and kinetic study. *Eur. J. Biochem.* 88:379–385.

51. Waugh, R. E. 1983. Effects of abnormal cytoskeletal structure on erythrocyte membrane mechanical properties. *Cell Motil.* 3:609–622.